




Measurement of the thermal neutron cross section and resonance integral of the $^{187}\text{Re}(n,\gamma)^{188}\text{Re}$ reaction

Thi Hien Nguyen^{1,3}, Van Do Nguyen^{2,3}, Guinyun Kim^{1,a} , Yong-uk Kye⁴,
Sung-Gyun Shin⁴, Moo-Hyun Cho⁴

¹ Department of Physics, Kyungpook National University, Daegu 41566, Korea

² Institute of Theoretical and Applied Research, Duy Tan University, 1 Phung Chi Kien Street, Hanoi 100000, Vietnam

³ Institute of Physics, Vietnam Academy of Science and Technology, 10 Dao Tan, Hanoi, Vietnam

⁴ Department of Advanced Nuclear Engineering, Pohang University of Science and Technology, Pohang 37673, Korea

Received: 2 December 2019 / Accepted: 17 April 2020 / Published online: 29 April 2020

© Società Italiana di Fisica and Springer-Verlag GmbH Germany, part of Springer Nature 2020

Abstract We measured the thermal neutron capture cross sections (σ_0) and resonance integral (I_0) of the $^{187}\text{Re}(n,\gamma)^{188}\text{Re}$ reaction relative to that of the $^{197}\text{Au}(n,\gamma)^{198}\text{Au}$ monitor reaction using neutron activation with the Cd ratio method. The investigated samples and monitors were irradiated with and without a 0.5-mm-thick Cd cover for the pulsed neutron source based on the 100-MeV electron linac at the Pohang Accelerator Laboratory (PAL). The induced activities for the reaction products were measured using a high-purity germanium (HPGe) detector. In order to improve the accuracy of the experimental results, the necessary corrections were made. The thermal neutron capture cross sections and resonance integral of the $^{187}\text{Re}(n,\gamma)^{188}\text{Re}$ reaction were determined relative to reference values of $\sigma_{o,\text{Au}} = 98.65 \pm 0.09$ barn and $I_{o,\text{Au}} = 1550 \pm 28$ barn from the $^{197}\text{Au}(n,\gamma)^{198}\text{Au}$ reaction, respectively. The corresponding values for the $^{187}\text{Re}(n,\gamma)^{188}\text{Re}$ reaction were determined to be $\sigma_{0,\text{Re}} = 75.6 \pm 3.4$ barn and $I_{0,\text{Re}} = 317 \pm 22$ barn, respectively. The obtained results are compared with the literature data and discussed.

1 Introduction

Naturally occurring rhenium (Re) consists of ^{185}Re with 37.4% abundance and a long-lived radioactive isotope ^{187}Re (half-life of 4.33×10^{10} years) with 62.6% abundance. Rhenium is a refractory metal with exceptional heat and abrasion resistance. Due to its special properties, rhenium and its alloys can be used in many applications, including reactor technology and jet engines [1–3]. The neutron capture reaction product of the $^{187}\text{Re}(n,\gamma)^{188}\text{Re}$ reaction is a high energy beta-emitting radioisotope ($E_{\beta,\text{max}} = 2.12$ MeV), which has been shown to be a very attractive candidate for use in medical applications [4–6]. Generally, the ^{188}Re isotope is produced from ^{186}W via two successive neutron capture reactions: $^{186}\text{W}(n,\gamma)^{187}\text{W}(n,\gamma)^{188}\text{W} \xrightarrow[T_{1/2=69.78d}]{\beta^-} ^{188}\text{Re}$ [5]. Therefore, the production of ^{188}Re directly through the

^a e-mail: gnkim@knu.ac.kr (corresponding author)

neutron capture reaction $^{187}\text{Re}(n,\gamma)^{188}\text{Re}$ is considered an alternative to the $^{188}\text{W}/^{188}\text{Re}$ generator system [6].

In order to determine the activity of the medical radioisotope ^{188}Re produced via the $^{187}\text{Re}(n,\gamma)^{188}\text{Re}$ reaction, accurate knowledge of the thermal and resonance integral cross sections is required. However, the existing reference data for the $^{187}\text{Re}(n,\gamma)^{188}\text{Re}$ reaction are still limited. In the literature, we have found seven articles on thermal neutron capture cross sections [7–13] and seven on resonance integrals [7, 8, 14–18]. All reference data are relatively old; the first measurement was carried out in 1947 [13], and the most recent one was in 1987 [7]. Most of the measurements were carried out between 1960 and 1980. The experimental data also show large discrepancies. The thermal neutron capture cross sections [7–13] vary from 55 ± 7 barn [9] to 88 ± 14 barn [10], a difference of about 60%. The resonance integrals [7, 8, 14–18] are in the range of 160 ± 18 barn [7] to 323 ± 20 barn [15], a difference of 102%. Obviously, a consistency problem exists among the measured cross sections of the $^{187}\text{Re}(n,\gamma)^{188}\text{Re}$ reaction. The reason may be partly attributed to the different experimental conditions. On the other hand, during the experimental process, the corrections have not been fully implemented. Therefore, for better data evaluations and/or applications, additional experimental data are required.

In this work, we measured the thermal neutron capture cross sections and resonance integral of the $^{187}\text{Re}(n,\gamma)^{188}\text{Re}$ reaction in thermal and epithermal neutron fields at the pulsed neutron facility of the Pohang Accelerator Laboratory (PAL). The measurements were performed with the foil activation method using a $^{197}\text{Au}(n,\gamma)^{198}\text{Au}$ monitor reaction. The induced activities for the irradiated foils were measured with a gamma spectrometer based on HPGe detector.

In this experiment, the necessary corrections for the losses due to gamma-ray attenuation, the dead time of the gamma counting spectrometer and the coincidence summing effect were made. In addition, correction factors for thermal neutron self-shielding (G_{th}) and epithermal neutron self-shielding (G_{epi}) as well as epithermal neutron shape factor (α) were also taken into account. Because of the thermal neutron cross section and resonance integral of both ^{187}Re and ^{197}Au are relatively high, their self-shielding effect significantly reduces the neutron flux in the sample, thereby reducing the number of nuclear reactions. Therefore, in order to ensure the values of self-shielding factors for the Re and Au foils, in this work, they are determined by both analytical and Monte-Carlo simulation. Finally, to confirm the present results, the obtained neutron capture cross section and resonance integral were compared with the previously measured [7–18] and evaluated [19–23] data.

2 Experimental details

2.1 Sample preparation and irradiation

Rhenium (Re, 99.98%, 0.1 mm thick), gold (Au, 99.95%, 0.03 mm thick), and indium (In, 99.95%, 0.05 mm thick) foils with the same size of $15 \text{ mm} \times 15 \text{ mm}$ were prepared for irradiation. The gold and indium metallic foils were used as the comparator reactions and the neutron flux monitors, respectively. The prepared samples were irradiated at the pulsed neutron facility based on the 100-MeV electron linac of the PAL. The pulsed neutrons were generated from a water-cooled Ta target via $\text{Ta}(\gamma, \text{xn})$ reactions, and the neutrons produced were slowed down in a cylindrical water moderator. Details of the pulsed neutrons including the production and thermalization of neutrons have been described elsewhere [24–26]. In this experiment, we set the water level at 5 cm above the water-cooled Ta target as shown in

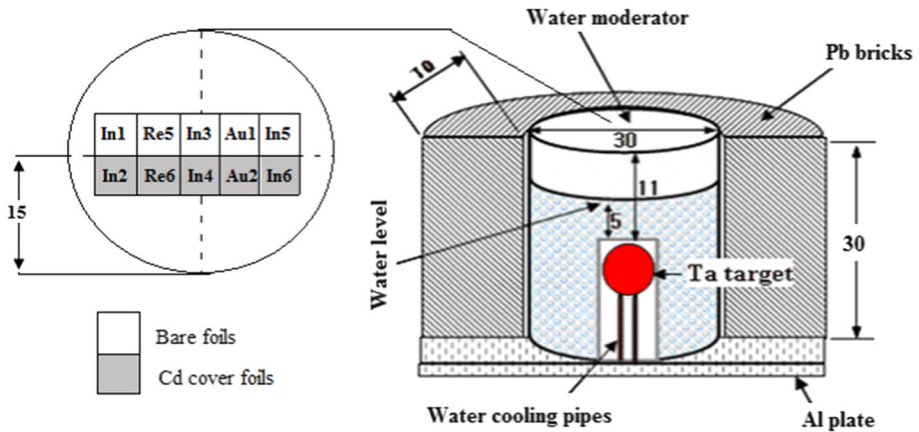


Fig. 1 Configuration of the pulsed neutron source based on the water-cooled Ta target and the water moderator system. Two sets of activation foils on the circular sample holder are arranged on the surface of the water moderator. The numbers in this figure refers to the dimensions in cm

Fig. 1. For irradiation, two sets of activation foils were used: one set was bare and the second set was wrapped in 0.5-mm-thick Cd. The foils were placed in the positions designated on the circular sample holder as shown in Fig. 1 and irradiated simultaneously on the top of the water moderator. Using this arrangement, neutron fluxes at the position of the rhenium and gold samples could be obtained by extrapolating the neutron flux measured at the indium positions. By preserving the configuration of the neutron source and keeping the water level at 5 cm above the surface of the Ta target, the neutron spectrum was checked and found that the shape of neutron spectra did not seem to change [27–29].

The irradiation was performed for 30 min with an electron energy of 65 MeV. During irradiation, the electron linac was operated with a repetition rate of 15 Hz, a pulse width of 1.2 μ s, and an electron beam current of 40 mA.

2.2 Measurement of γ -ray spectra

The γ -ray spectra from the activated foils were measured with a HPGe detector (ORTEC-GEM-20180-p) coupled to a PC-based multichannel analyser. The photopeak area in the resulting γ -ray spectra was analysed with GammaVision version 5.10. The detector efficiency was 20% relative to a 3-inch diameter \times 3-inch length NaI(Tl) detector and the energy resolution was 1.8-keV full width at half maximum (FWHM) at the 1332.5 keV γ -ray peak of ^{60}Co . The absolute photopeak efficiency for the HPGe detector was calibrated with γ -rays of known energy and intensity with standard gamma sources as described in the literature [29].

The nuclear reactions to be investigated and the characteristics of the induced radionuclides are given in Table 1 [30]. The activities of the ^{188}Re , ^{198}Au and $^{116\text{m}}\text{In}$ were measured using their strongest γ -rays of 155.04 keV (15.49%), 411.8 keV (95.62%) and 1293.56 keV (84.8%), respectively. The measurement of the irradiated foil was repeated several times based on the half-life of each radioactive isotope. For all measurements, the dead times were kept below 5% by changing the distance from the sample to the detector. The measurement time was extended to increase the statistics, so that the statistical error was <1%. A typical γ -ray spectrum for the irradiated Re foil is shown in Fig. 2.

Table 1 Nuclear spectroscopic data for the determination of the γ -ray activities [30]

Nuclear reaction	Half-life, $T_{1/2}$	Main γ -ray energy and intensity		Isotopic abundance (%)
		Energy (keV)	Intensity (%)	
$^{187}\text{Re} (n,\gamma)^{188}\text{Re}$	17.005 h	155.04*	15.49	62.6
		478.00	1.076	
		633.03	1.37	
		829.47	0.444	
$^{197}\text{Au} (n,\gamma)^{198}\text{Au}$	2.6941 days	411.80*	95.62	100
		675.88	0.805	
$^{115}\text{In} (n,\gamma)^{116\text{m}}\text{In}$	54.29 min	1097.28	58.5	95.71
		1293.56*	84.8	

*The gamma-rays, which are used in measurements

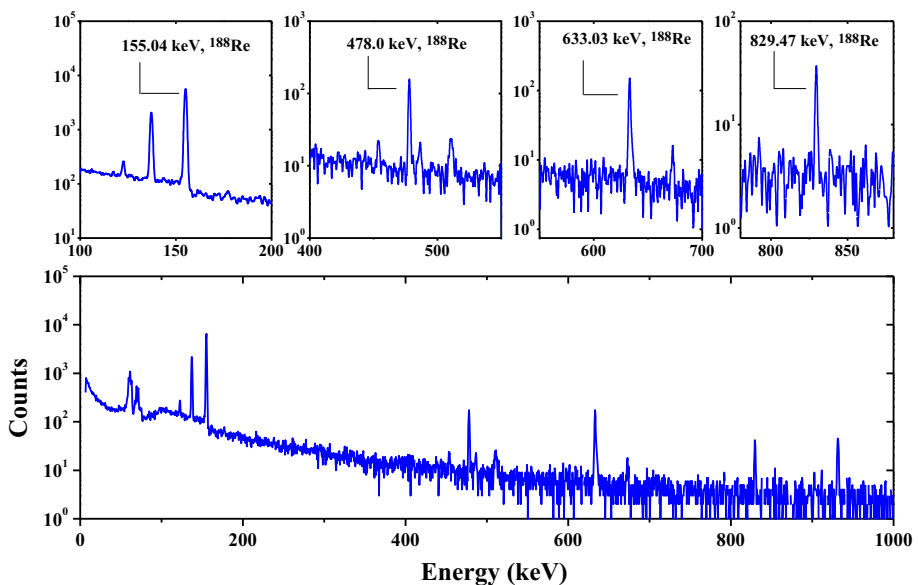


Fig. 2 A typical γ -ray spectrum from an irradiated Re foil with an irradiation time of 30 min, waiting time of 1800 min, and measuring time of 60 min

All γ -rays selected for activity measurements from ^{188}Re , ^{198}Au , and $^{116\text{m}}\text{In}$ were well separated and interference-free with relatively high intensity. Therefore, the error caused by γ -ray interference could be neglected. However, the counting losses caused by the attenuation effect from the 155.04 keV γ -ray of ^{188}Re , the 411.8 keV γ -ray of ^{198}Au , and the 1293.56 keV γ -ray of $^{116\text{m}}\text{In}$ were corrected based on the attenuation factor. For a given γ -ray, the attenuation factor was approximated as follows: $f_{\text{att}} = (1 - e^{-\mu d}) / \mu d$, where μ is the linear attenuation coefficient (cm^{-1}) and d is the thickness of the foil sample (cm). The determined attenuation factor for the 155.04 keV γ -ray of the ^{188}Re foil is 0.912, that for the 411.8 keV γ -ray of the ^{198}Au foil is 0.945, and that for the 1293.56 keV γ -ray of the $^{116\text{m}}\text{In}$

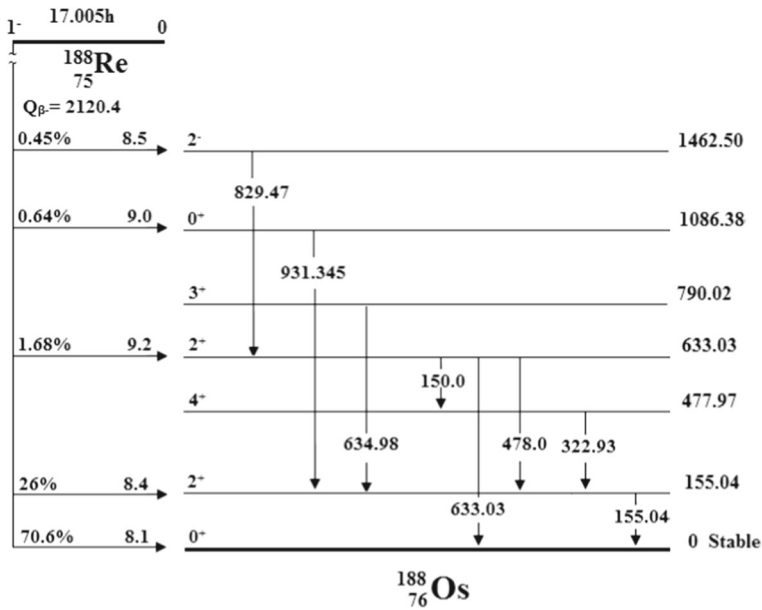


Fig. 3 Decay scheme of ^{188}Re

foil is 0.999. The activity without attenuation can be calculated by dividing the measured value by the attenuation factor.

The ^{188}Re radionuclide is a multi-gamma-ray emitter as shown in Fig. 3. The γ -rays emitted in a cascade can cause counting losses due to the coincidence summing effect. We can see the 155.04 keV γ -ray in a cascade with multiple γ -rays such as the 478.0-, 633.03-, 829.47-, and 931.34-keV γ -rays in Fig. 3. In addition, the 155.04 keV γ -ray is in a triple cascade with two γ -rays of 478.0 keV and 829.47 keV (three γ -rays are in cascade). In principle, the summing effect increases or decreases the counting loss at the 155.04 keV photopeak, i.e. the observed count numbers are less than the result if there is no cascading effect. This is known as summing-out. In order to decrease the contribution of the summing coincidence effect, the measurements were performed at the farthest possible geometry. In our measurements, the irradiated foils were positioned at 5 cm and/or 10 cm from the surface of the detector, depending on their activities. In addition, to adjust for the counting number lost from the full energy peak of the 155.04 keV γ -ray, we also applied a correction for the coincidence summing effect. The correction factor for the coincidence summing effect is defined as the ratio of the count rates without coincidence to those with coincidence. In this work, the correction factor, C_c , was approximated as follows [31]:

$$C_c = \frac{1}{1 - \sum_{i=1}^{i=j} I(E_i) \cdot \varepsilon_t(E_i)} \tag{1}$$

where $I(E_i)$ is the intensity (or fraction) of coincidence γ -rays for energy E_i coincident with the γ -ray of interest, and $\varepsilon_t(E_i)$ is the total efficiency of the coincidence γ -ray for energy E_i .

The calculated results show that for the measurements made at a distance of 10 cm from the detector, the summing-out (coincidence) correction factor for the 155.04 keV photopeak is negligible, less than 1.0007 for any cascading γ -ray. If the measurements are performed at 5 cm, the correction factors are also very small. In this case, the highest correction factor

belongs to the cascading γ -rays of 155.04 keV and 478.0 keV at approximately 1.003. This correction factor is approximately the same as that of the triple cascading γ -rays, including the 155.04 keV, 478.0 keV, and 829.47 keV γ -rays. Obviously, the counting losses due to coincidence summing effects do not considerably affect the counting numbers of the 155.04 keV photopeak. This is because the intensity of the cascading γ -rays is low (0.01–0.5%), except that of the 478.0 keV γ -ray (1.076%). In practice, we ignored the contribution of the coincidence summing effects in the activity measurement of ^{188}Re based on the 155.04 keV γ -ray.

3 Data analysis

3.1 Measurement of the thermal neutron cross sections

The thermal neutron capture cross sections of the $^{187}\text{Re}(n,\gamma)^{188}\text{Re}$ reaction, $\sigma_{0,\text{Re}}$, was determined relative to that of the $^{197}\text{Au}(n,\gamma)^{198}\text{Au}$ reaction as follows [32, 33]:

$$\sigma_{0,\text{Re}} = \sigma_{0,\text{Au}} \times \frac{R_{\text{Re}} - F_{\text{Re,Cd}}R_{\text{Re,Cd}}}{R_{\text{Au}} - F_{\text{Au,Cd}}R_{\text{Au,Cd}}} \times \frac{G_{\text{th,Au}}}{G_{\text{th,Re}}} \times \frac{g_{\text{Au}}}{g_{\text{Re}}}, \tag{2}$$

where $\sigma_{0,\text{Au}} = 98.65 \pm 0.09$ barn, and R_x and $R_{x,\text{Cd}}$ refer to the reaction rates per atom for the given sample x (Re or Au) irradiated without and with a Cd cover. $F_{x,\text{Cd}}$ is the Cd correction factor for a given element x irradiated under a Cd cover, where $F_{\text{Re,Cd}} = 1.000$ [34] and, $F_{\text{Au,Cd}} = 1.009$ [34]. $G_{\text{th},x}$ is the thermal neutron self-shielding factor for a given element x . For a thin activation foil, the calculation was performed using the analytical formula given in the literature [35], giving $G_{\text{th,Re}} = 0.991 \pm 0.031$ and $G_{\text{th,Au}} = 0.990 \pm 0.025$. The Westcott factor for the $^{187}\text{Re}(n,\gamma)^{188}\text{Re}$ reaction was $g_{\text{Re}} = 0.9942$ [36], and that for the $^{197}\text{Au}(n,\gamma)^{198}\text{Au}$ was $g_{\text{Au}} = 1.0054$ [36].

The reaction rates per atom for the sample x (Re or Au) irradiated with Cd cover ($R_{x,\text{Cd}}$) or without Cd cover (R_x) was determined as follows [37]:

$$R_{x,\text{Cd}} \text{ or } R_x = \frac{S_\gamma \lambda (1 - e^{-\lambda t_{cp}})}{N_o \varepsilon_\gamma I_\gamma (1 - e^{-\lambda \tau})(1 - e^{-\lambda t_i})e^{-\lambda t_w}(1 - e^{-\lambda t_m})}, \tag{3}$$

where S_γ is the net number of counts under the photopeak collected during the measurement time t_m and N_o is the number of target nuclei. The factors ε_γ and I_γ are the detector efficiency and the absolute intensity of the γ -ray, λ is the decay constant of the isotope, t_i and t_w are the irradiation and the waiting time, τ is the pulse width, and t_{cp} is the cycle period.

3.2 Measurement of the resonance integral

The epithermal neutron spectrum of the Pohang electron linac-based neutron source corresponds to the form $1/E^{1+\alpha}$, where α is an energy-independent epithermal neutron spectrum shape factor. Therefore, we measured the resonance integral $I_0(\alpha)$ instead of I_0 . The conversion of I_0 for an ideal $1/E$ epithermal neutron spectrum to $I_0(\alpha)$ for a $1/E^{1+\alpha}$ real epithermal neutron spectrum takes the form [32, 33]:

$$I_0(\alpha) = (1\text{eV})^\alpha \left[\frac{I_0 - 0.429g\sigma_0}{(\bar{E}_r)^\alpha} + \frac{0.429g\sigma_0}{(2\alpha + 1)(E_{Cd})^\alpha} \right], \tag{4}$$

where $I_{0,\text{Au}} = 1550 \pm 28$ barn, \bar{E}_r (eV) is the effective resonance energy with $\bar{E}_r = 39.35$ for $^{187}\text{Re}(n,\gamma)^{188}\text{Re}$ reaction [38] and $\bar{E}_r = 4.9$ eV for $^{197}\text{Au}(n,\gamma)^{198}\text{Au}$ reaction [38], respec-

Table 2 Self-shielding correction factors and some key parameters used to estimate the G_{th} and G_{epi}

Nuclear reaction	\bar{E}_r (eV) [38]	Γ_γ (eV) [38]	Γ_n (eV) [38]	Analytical method		MCNPX simulation	
				G_{th}	G_{epi}	G_{th}	G_{epi}
$^{187}\text{Re}(n,\gamma)^{188}\text{Re}$	39.35	55.0	5.98	0.991 ± 0.031	0.722 ± 0.022	0.962	0.695
$^{197}\text{Au}(n,\gamma)^{198}\text{Au}$	4.9	0.1225	0.0148	0.990 ± 0.025	0.299 ± 0.008	0.950	0.320

tively, $E_{cd} = 0.55$ eV is the effective Cd cut-off energy and the shape of the epithermal neutron spectrum $\alpha = 0.068 \pm 0.004$. The term $(I_0 - 0.429g\sigma_0)$ represents the reduced resonance integral, i.e. with the $1/v$ tail subtracted. However, it should be noted that Eq. (4) applies only to the thermal neutron energy, $E_0 = 0.0253$ eV and the Cd cut-off energy, $E_{cd} = 0.55$ eV, so that we can obtain $2\sqrt{E_0/E_{cd}} = 0.429$.

The measured resonance integral value $I_{0,Re}(\alpha)$ for the $^{187}\text{Re}(n,\gamma)^{188}\text{Re}$ reaction can be obtained relative to that of the monitor reaction $^{197}\text{Au}(n,\gamma)^{198}\text{Au}$ as follows [32, 33]:

$$I_{0,Re}(\alpha) = I_{0,Au}(\alpha) \times \frac{g_{Re}\sigma_{0,Re}}{g_{Au}\sigma_{0,Au}} \times \frac{CR_{Au} - F_{Au,Cd}}{CR_{Re} - F_{Re,Cd}} \times \frac{G_{epi,Au}}{G_{th,Au}} \times \frac{G_{th,Re}}{G_{epi,Re}}. \tag{5}$$

Most of the symbols and coefficients in Eq. (5) were introduced in previous formulas. $CR_x = (R_x/R_{x,Cd})$ is the Cd ratio for the x -sample or monitor ($CR_{Au} = 2.76 \pm 0.04$ and $CR_{Re} = 3.85 \pm 0.08$), and $G_{epi,x}$ is the self-shielding factor of epithermal neutrons for a given element. The neutron self-shielding factor $G_{epi,x}$ is calculated according to the analytical formula given in ref [39], yielding $G_{epi,Re} = 0.722 \pm 0.022$ and $G_{epi,Au} = 0.299 \pm 0.008$.

3.3 Simulation of neutron self-shielding correction factors

The specific activity of reaction products with a large neutron capture and resonance integral cross sections such as ^{187}Re and ^{197}Au nuclides is significantly reduced by both the thermal and epithermal self-shielding effects. In this work, the neutron self-shielding correction factors were estimated through analytical calculations [35, 39]. We also simulated the self-shielding effect using the Monte Carlo N-Particle extended (MCNPX) code [40–42] in order to validate the analytical results. We compared the self-shielding correction factors from both the analytical and the MCNPX simulation methods. The self-shielding correction factor is defined as the ratio of the neutron flux in the sample to that in a similar and infinitely diluted sample. In the Monte Carlo simulation, the neutron fluxes in the foil samples were simulated with MCNPX code [43] using the track length estimation tool (F4). The neutron capture cross sections were taken from the JEFF 3.1 library [20]. The neutron energies were classified into two ranges, one from 1.0 meV to 0.55 eV for thermal neutrons, and the other from 0.55 eV to 12 MeV for epithermal neutrons.

The G_{th} and G_{epi} factors obtained from both the analytical method and the MCNPX code along with some of the key parameters used to estimate their values such as the resonance energy E_{res} and the resonance widths Γ_γ and Γ_n for the (n,γ) and (n,n) reactions [38] are given in Table 2. For the $^{187}\text{Re}(n,\gamma)^{188}\text{Re}$ reaction, the G_{th} values obtained from two independent methods differed by 2.9%, while the G_{epi} values differed by 3.7%. For the $^{197}\text{Au}(n,\gamma)^{198}\text{Au}$ reaction, these values were 4% and 6.57%, respectively.

Table 3 Thermal neutron capture cross sections and resonance integral of $^{187}\text{Re}(n,\gamma)^{188}\text{Re}$ reaction obtained from the present study with other measurements and evaluations

References	σ_0 (b)	% Diff. σ_0^*	I_0 (b)	% Diff. I_0^*	Monitor
This work	75.6 ± 3.4		317 ± 22		Au
Trofimov [7]	80 ± 10	- 5.83	160 ± 18	49.53	Au, In, U
Heft [8]	75 ± 1	0.78	318 ± 50	- 0.32	U, Sc, Au, Co
Van der Linden et al. [14]	-		311 ± 30	1.89	Au
Pierce et al [15]	-		323 ± 20	- 1.89	Au
Sher et al [16]	-		308 ± 20	2.84	Au
Takahashi et al. [9]	55 ± 7	27.24	-		-
Karam et al. [10]	88 ± 14	- 16.42	-		Au
Lyon [11]	67	11.36	-		Co
Macklin et al. [17]	-		305	3.79	Au
Pomerance [12]	63 ± 5.04	16.66	-		Au
Harris et al. [18]	-		275	13.25	Au
Seren et al. [13]	75.3 ± 15.6	0.38	-		-
ENDF/B-VII.1 [19]	76.71	- 1.48	300	5.36	-
JEFF 3.1.2 [20]	76.71	- 1.48	294.3	7.16	-
ROSFOND-2010 [21]	76.71	- 1.48	298.1	5.96	-
EAF-2010 [22]	74.84	- 1.65	287.4	9.34	-
Mughabghab [23]	76.4 ± 1	- 1.07	300 ± 20	5.36	-
Experimental weighted mean only	75.31 ± 0.69	0.37	$310.75 \pm 10.53^{**}$ $272.29 \pm 9.09^{***}$	2.21 14.19	

*% Diff. means that the percentage difference = $100 * (1 - \text{literature value/present value})$

**Weighted average resonance integral value does not include Trofimov's result

***Weighted average resonance integral value includes Trofimov's result

4 Results and discussion

The thermal neutron capture and resonance integral cross sections of the $^{187}\text{Re}(n,\gamma)^{188}\text{Re}$ reaction were measured relative to the corresponding values of $\sigma_0 = 98.65 \pm 0.09$ barn and $I_0 = 1550 \pm 28$ barn for the $^{197}\text{Au}(n,\gamma)^{198}\text{Au}$ reaction [44]. The results obtained in this study together with the related literature data are summarized in Table 3 and plotted in Figs. 4 and 5. The values listed in Table 3 include both the measured and evaluated data.

The main sources of experimental uncertainties are listed in Table 4. The uncertainties for the thermal neutron capture cross-sectional measurements for the $^{187}\text{Re}(n,\gamma)^{188}\text{Re}$ reaction are mainly from the detector efficiency, γ -ray intensity, and thermal neutron shielding factor. The main sources of uncertainty in the resonance integral measurements are the α -shape factor, Cd ratio, and detector efficiency. The total uncertainties for the thermal neutron capture cross sections and resonance integral for the $^{187}\text{Re}(n,\gamma)^{188}\text{Re}$ reaction were determined to be 4.41% and 7.16%, respectively.

The experimental neutron capture cross sections listed in Table 3 range from 55 ± 7 barn [9] to 88 ± 14 barn [10]. Obviously, there are significant differences between the literature data. The obtained result of 75.6 ± 3.4 barn is within 0.78% (1σ) of the measurements by

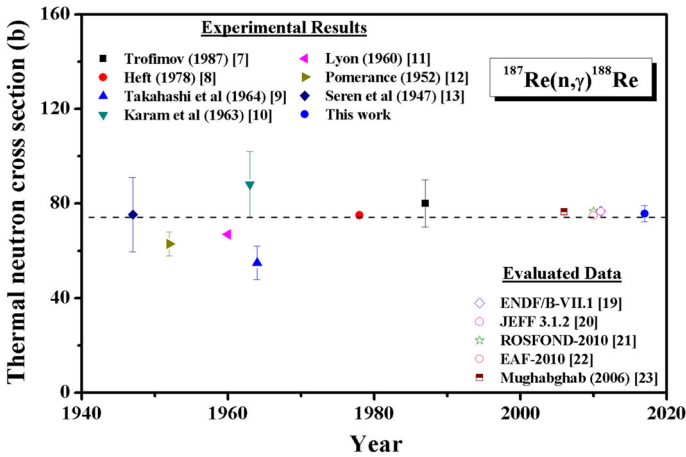


Fig. 4 Comparison of thermal neutron capture cross sections of the $^{187}\text{Re}(n,\gamma)^{188}\text{Re}$ reaction

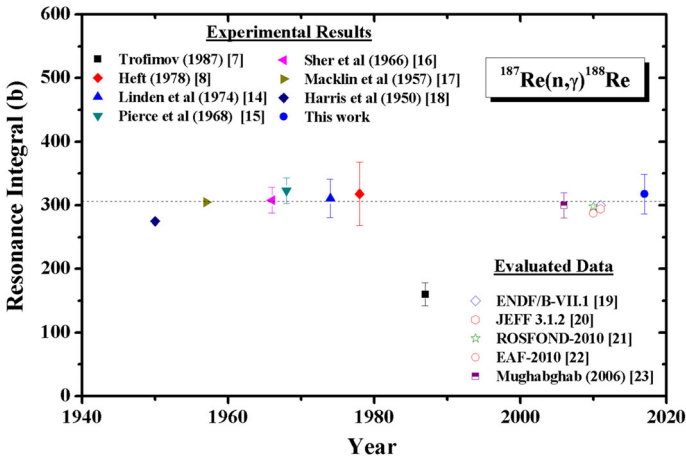


Fig. 5 Comparison of resonance integrals of the $^{187}\text{Re}(n,\gamma)^{188}\text{Re}$ reaction

Helf [8] and Seren et al. [16], but disagrees with the results reported by other authors by 5.8% [7] to 27.3% [9]. The results are also in good agreement with the evaluated values, with differences in the range of 1.48-1.65%. This comparison shows that the thermal neutrons capture cross section obtained in this study represents a good average of the values reported thus far.

The reported resonance integral values are distributed in a wide range, from 160 ± 18 barn [7] to 323 ± 20 barn [15]. The resonance integral in this work is within 3.79% (1σ) of most of the reported data, specifically that of Heft [8], Van der Linden et al [14], Pierce et al. [15], Sher et al. [16] and Macklin et al. [17]. The value differs by 13.25% from the measurement obtained by Harris et al. [18] and by 49.5% from the experimental result reported by Trofimov [7]. The value also agrees well with a weighted average of the reported values that does not include the measurement by Trofimov [7], with a difference of only about 2.21% (see Table 3).

Table 4 Estimated uncertainties for measured thermal neutron and resonance integral cross sections

Sources of uncertainty	Uncertainties (%)	
	^{198}Au	^{188}Re
<i>Thermal neutron cross-sections</i>		
Counting statistics	0.6	0.8
Geometry	0.55	0.55
Detection efficiency	2.80	2.80
Mass of foil weight	0.10	0.10
Half-life	0.01	0.13
Gamma-ray intensity	–	0.38
Thermal neutron self-shielding factor	0.85	0.9
Reference thermal neutron cross section	0.09	–
Attenuation effect	0.2	0.4
Sub-total experimental uncertainty	3.05	3.19
Total experimental uncertainty	4.41	
<i>Resonance integral measurements</i>		
Epithermal neutron self-shielding factor	1.79	2.81
Thermal neutron shielding factor	0.85	0.9
Reference thermal neutron cross section	0.09	1.90
Reference resonance integral	1.81	–
Cadmium ratio	1.50	2.25
α -Shape factor	3.5	3.5
Sub-total experimental uncertainty	4.66	5.44
Total experimental uncertainty	7.16	

The comparisons confirm that the current resonant integral is a good reflection of the average of the experimental results that exist thus far in the literature.

Finally, to confirm the applicability of the neutron self-shielding correction factors obtained with two independent methods, we applied the self-shielding correction factors obtained with the MCNPX code to calculate the thermal neutron capture and resonance integral cross sections for the $^{187}\text{Re}(n,\gamma)^{188}\text{Re}$ reaction for comparison. The obtained results were $\sigma_{0,\text{Re}} = 74.4 \pm 3.3$ barn and $I_{0,\text{Re}} = 332 \pm 23$ barn, respectively. The thermal neutron capture cross sections and resonance integrals obtained by applying the self-shielding factors determined from two independent methods differed by 1.5% and 4.8%, respectively. The comparisons confirmed that there is consistency between the self-shielding factors obtained using the analytical and MCNPX simulation methods, because both the thermal neutron cross section and the resonance integral values calculated on the basis of the self-shielding parameters obtained with the two methods are still in good agreement, with differences within a 1σ limit.

5 Summary

The thermal neutron capture cross sections and the resonance integral of the $^{187}\text{Re}(n,\gamma)^{188}\text{Re}$ reaction were determined to be 75.6 ± 3.4 barn and 317 ± 22 barn, respectively. The measurements were carried out relative to the $^{197}\text{Au}(n,\gamma)^{198}\text{Au}$ monitor reaction. To obtain the highest

possible accuracy for the experimental results, the necessary corrections for counting losses were made. In order to validate the neutron self-shielding correction factors, Monte Carlo simulations were performed to cross-check the analytical results. The obtained thermal neutron captures and resonance integral cross sections of the $^{187}\text{Re}(n,\gamma)^{188}\text{Re}$ reaction are very close to the weighted average of the relevant reference data. This conformity demonstrates the validity of the present experimental procedure and the method used. The obtained results appear reliable for use in calculating the activity of the ^{188}Re medical isotope generated by the $^{187}\text{Re}(n,\gamma)^{188}\text{Re}$ reaction.

Acknowledgements The authors would like to thank the staff of the electron linac at the Pohang Accelerator Laboratory (PAL), Korea, for the excellent operation of the electron linac and their support during the experiment. This research was supported by the National Research Foundation of Korea through a grant provided by the Ministry of Science, ICT and Future Planning (NRF-2017R1D1A1B03030484, NRF-2013M7A1A1075764), by the Collaboration for Leadership in Applied Health Research and Care - Greater Manchester (GB) (NRF-2018R1A6A1A06024970), and by the Vietnam National Foundation for Science and Technology Development (NAFOSTED) under Grant No. 103.04-2018.314.

Data Availability Statement This manuscript has associated data in a data repository. [Authors' comment: All data used in this paper are deposited in the EXFOR library and the data generated during this study will be deposited in the same library].

References

1. G. Leinweber, R.C. Block, B.E. Epping, D.P. Barry, M.J. Rapp, Y. Danon, T.J. Donovan, S. Landsberger, J.A. Burke, M.C. Bishop, A. Youmans, G.N. Kim, M.W. Lee, N.J. Drindak, EPJ Web of Conf. **146**, 11003 (2017)
2. B.E. Epping, G. Leinweber, D.P. Barry, M.J. Rapp, R.C. Block, T.J. Donovan, Y. Danon, S. Landsberger, Prog. Nucl. Energy **99**, 59 (2017)
3. J.T. Busby, K.J. Leonard, S.J. Zinkle, J. Nucl. Mater. **366**, 388 (2008)
4. N. Lepareur, F. Laccueille, C. Bouvry, F. Hindré, E. Garcion, M. Chérel, N. Noiret, E. Garin, F.F.R. Knapp Jr., Front. Med. **6**, 132 (2019)
5. J. Mukiza, E. Byamukama, J. Sezirahiga, K.N. Ngbolua, V. Ndebwanimana, Rwanda. Med. J. **75**, 14 (2018)
6. A. Boschi, L. Uccelli, M. Pasquali, A. Duatti, A. Taibi, G. Pupillo, J. Esposito, J. Chem. **2014**, 14 (2014)
7. Y.N. Trofimov, Voprocj Atomnoj Nauki i Tehniki, Ser.: Yadernye Konstanty. **4**, 10 (1987)
8. R.E. Heft, A consistent set of nuclear-parameter values for absolute instrumental neutron activation analysis, in *Proceedings of the American Nuclear Society Topical Conference on Computers in Activation Analysis and Gamma-Ray Spectroscopy, Mayaguez, Puerto Rico 1978* (National Technical Information Service, U.S. Dept. of Commerce, 1979), p. 495
9. K. Takahashi, M. McKeown, G.S. Chaff-Goldhaber, Phys. Rev. **136**, B18 (1964)
10. R.A. Karam, T.F. Parkinson, M.F. Panczyk, in *The Nuclear Properties of Rhenium*, Florida. University, Gainesville Report No. NP-12519 (1963)
11. W.S. Lyon, J. Nucl. Sci. Eng. **8**, 378 (1960)
12. H. Pomerance, Phys. Rev. **88**, 412 (1952)
13. L. Seren, H.N. Friedlander, S.H. Turkey, Phys. Rev. **72**, 888 (1947)
14. R. Van Der Linden, F. De Corte, J. Hoste, J. Radioanal. Chem. **20**, 695 (1974)
15. C.R. Pierce, D.F. Shook, D. Bogart, *Resonance Integrals of Rhenium for a Wide Range of Sample Sizes* (National Aeronautics and Space Administration, Washington, D.C., 1968)
16. R. Sher, L.L. Sage, T.J. Connolly, H.L. Brown, Trans. Am. Nucl. Soc **9**, 248 (1966)
17. R.L. Macklin, N.H. Lazar, W.S. Lyon, Phys. Rev. **107**, 504 (1957)
18. S.P. Harris, C.O. Muehlhause, G.E. Thomas, Phys. Rev. **79**, 11 (1950)
19. M.B. Chadwick, I.J. Thompson, A. Trkov, R.L. Vogt, S.C. van der Marck, A. Wallner, M.C. White, D. Wiarda, P.G. Young, Nucl. Data Sheets **112**, 2887 (2011)
20. A.J. Koning, E. Bauge, C.J. Dean, E. Dupont, U. Fischer, R.A. Forrest, R. Jacqmin, H. Leeb, M.A. Kellett, R.W. Mills, C. Nordborg, M. Pescarini, Y. Rugama, P. Rullhusen, J. Korean Phys. Soc **59**, 1057 (2011)

21. S.V. Zabrodskaia, *ROSFOND-Russia national library of evaluated neutron data, problems of atomic science and technology* **2**, 2005 (2005)
22. J.C. Sublet, L.W. Packer, J. Kopecky, R.A. Forrest, A.J. Koning, D.A. Rochman, *The European Activation File: EAF-2010 Neutron-Induced Cross-Sections Library*, EASY Doc. Ser. CCFE-R 10 (2010)
23. S.F. Mughabghab, *Thermal Neutron Capture Cross-Sections, Resonance Integrals and g-Factor* (Brookhaven National Laboratory, Suffolk County, 2006)
24. G.N. Kim, Y.S. Lee, V. Skoy, V. Kovalchuk, *J. Korean Phys. Soc.* **38**, 14 (2001)
25. G.N. Kim, V. Kovalchuk, Y.S. Lee, V. Skoy, M.H. Cho, I.S. Ko, W. Namkung, D.W. Lee, H.D. Kim, S.K. Ko, S.H. Park, D.S. Kim, T.I. Ro, Y.G. Min, *Nucl. Inst. Methods A* **485**, 458 (2002)
26. K. Devan, A.K.M.M.H. Meaze, G.N. Kim, Y.S. Lee, H. Kang, M.H. Cho, I.S. Ko, W. Namkung, N.V. Do, P.D. Khue, T.D. Thiep, P.V. Duan, *J. Korean Phys. Soc.* **49**, 89 (2006)
27. N.T. Hien, G.N. Kim, K.S. Kim, N.V. Do, P.D. Khue, K.T. Thanh, S.G. Shin, M.H. Cho, *Nucl. Inst. Methods B* **424**, 37 (2018)
28. N.V. Do, P.D. Khue, K.T. Thanh, N.T. Hien, G.N. Kim, K.S. Kim, S.G. Shin, Y.U. Kye, M.H. Cho, *Radiat. Phys. Chem.* **139**, 109 (2017)
29. N.V. Do, P.D. Khue, K.T. Thanh, N.T. Hien, G.N. Kim, K.S. Kim, S.G. Shin, M.H. Cho, M. Lee, *Nucl. Inst. Methods B* **362**, 9 (2015)
30. NuDat 2.6, National Nuclear Data Center, Brookhaven National Laboratory, updated 2011, available from <http://www.nndc.bnl.gov/>. (Table of Radioactive isotopes)
31. D.M. Montgomery, G.A. Montgomery, *J. Radioanal. Nucl. Chem.* **193**, 71 (1995)
32. N.V. Do, P.D. Khue, K.T. Thanh, L.T. Son, *Nucl. Inst. Methods B* **266**, 21 (2008)
33. M. Karadag, H. Yucel, M. Tan, A. Ozmen, *Nucl. Inst. Methods A* **501**, 524 (2003)
34. F. De Corte, A. Simonits, A. De Wispelaere, *J. Radioanal. Nucl. Chem.* **133**, 131 (1989)
35. M. Blaauw, *Nucl. Inst. Methods A* **356**, 403 (1995)
36. S.F. Mughabghab, *Thermal Neutron Capture Cross-Sections, Resonance Integrals and g-Factor* (Brookhaven National Laboratory, Suffolk County, 2003)
37. V. Do Nguyen, D.K. Pham, D.T. Tran, *J. Korean Phys. Soc.* **48**, 382 (2006)
38. F. De Corte, A. Simonits, *At. Data Nucl. Data Tables* **85**, 47 (2003)
39. E. Martinho, I.F. Gonçalves, J. Salgado, *Appl. Radiat. Isot.* **58**, 371 (2003)
40. T.E. Booth, J.F. Briesmeister, D.G. Collins, J.J. Devaney, G.P. Estes, H.M. Fisher, R.A. Forster, T.N.K. Godfrey, J.S. Hendricks, H.G. Hughes, R.C. Little, R.E. Prael, R.G. Schrandt, R.E. Seamon, E.C. Snow, W.L. Thompson, W.T. Urban, J.T. West, *MCNP-A General Monte Carlo Code for Neutron and Photon Transport LA—7396-M-DE87 000708* (Los Alamos National Laboratory, New Mexico, 1986)
41. I.F. Gonçalves, E. Martinho, J. Salgado, *Appl. Radiat. Isot.* **56**, 945 (2002)
42. P. Panikkath, P. Mohanakrishnan, *Eur. Phys. J. A* **52**, 276 (2016)
43. S.H. Jonh, W.M. Gregg, L.F. Michael, R.J. Michael, C.J. Rusell, W.D. Joe, P.F. Joshua, B.P. Denise, S.W. Laurie, M.J. William, *MCNPX 2.6.0*, LANL Report LA-UR-08-2216, Los Alamos, (2008) <http://mcnpx.lanl.gov/>.
44. S.F. Mughabghab, *Neutron Cross-Sections*, vol. 1, 4th edn. (Academic Press, New York, 1984)